

# Microwave Diagnostics for Investigation of Long Spark and Artificial Charged Aerosol Cloud

Nikolay Bogatov<sup>1,\*</sup>, Vladimir Syssoev<sup>1,2</sup>, Dmitry Suharevsky<sup>1,2</sup>, Marat Bulatov<sup>1,2</sup>, Michail Andreev<sup>2</sup>, Alexander Kostinsky<sup>1,3</sup>, Eugene Mareev<sup>1</sup> and Vladimir Rakov<sup>1,4</sup>

1. Institute of Applied Physics RAS, Nizhny Novgorod, Russian Federation
2. High-Voltage Research Centre VEI, Istra, Moscow region, Russian Federation
3. Higher School of Economics, Moscow, Russian Federation
4. Department of Electrical and Computer Engineering, University of Florida, Gainesville, Florida, USA

**ABSTRACT:** Presented is the project of the microwave diagnostics, intended for measuring the absolute value and dynamics of space-averaged conductivity of plasma in the streamer zone and the sheath of a long spark and plasma inside the artificial charged aerosol cloud during a discharge process. The first results of artificial charged aerosol cloud discharges investigation with use of the microwave diagnostics are obtained. By weakening the probing microwave radiation was measured absolute value and dynamics of space-averaged electron density in the cloud during discharges initiated by grounded metal ball.

## INTRODUCTION

Lightning and her lab analog - spark - remain poorly understood, despite their many years of intensive research. In particular, there are practically no measurements of nonequilibrium plasma parameters of spark discharges, which is the plasma of leaders and streamers. There no any experimental evidence for the existence of the streamer corona at the edge of return stroke ionization wave which should collect charge from the leader sheath to the channel. All experimental methods for studying lightning and sparks (except Schlieren method used, for example, in [Les Renardieres Group 1977]) still have been passive – they are electrical measurements (measurements of voltage and current to the electrodes and the electric field in the vicinity of grounded surfaces) and registration of discharges radiation.

In this paper we propose to use an active method of investigation of spark discharges plasma by microwave radiation probing. For low temperature and low electron density plasma as it is in streamers and leaders the main plasma effect on microwaves is absorption and phase shift. In this case the measuring of relative probing microwaves attenuation or phase shift allows one to directly find the electron density averaged over the volume occupied by the plasma inside the microwave beam. In the other case of high temperature and high electron density, proper to spark channel at the main stage of a discharge, the main contribution to the probing microwave attenuation make reflection on the plasma boundary. When

---

\* Contact information: Nikolay Bogatov, Institute of Applied Physics RAS, Nizhny Novgorod, Russian Federation, Email: bogatov@appl.sci-nnov.ru

simultaneous presence of both plasma types in the microwave beam the effects of absorption and reflection can be divided by measuring of relative intensity both passing and reflected microwaves.

### MICROWAVE DIAGNOSTICS OF THE LONG SPARK

Diagnostic microwave radiation should be directed to the object in the form of a beam of electromagnetic waves. Microwave generator should be placed in a shielded building ("Control Room") for reasons of safety and noise immunity. The distance from the control room to spark is 90 meters. Transportation of microwave radiation to the stand with the spark discharge through waveguides is impossible because too large losses in waveguides (in a rectangular waveguide 8 mm range - 0.6 dB/m, coaxial - substantially more). The only means of delivery of microwave radiation to the object under study is a quasi-optical system. In the quasi-optical system of millimeter waves range can be used metal mirrors and dielectric lens. Nearest to the spark discharge quasi-optical elements must be dielectric, since they are located at a distance from the spark discharge comparable with the distance between the electrodes and being metal might perturb an electrical field discharge gap and attract the spark discharges. All other elements of the quasi-optical focusing tract also advisable to make dielectric lenses due to lower manufacturing costs and greater ease of operation. As a material for the lens selected low-pressure polyethylene, as this material has the lowest among the known material dielectric dissipation at frequencies of 30 - 40 GHz .

The calculation was performed for the quasi-optical system of a Gaussian beam. The calculation was made of several quasi-optical systems and eventually was chosen that shown in Figure 1. Lens parameters are given in Table 1 ( $D$  is the diameter,  $F$  is the focal length,  $R$  is the radius of curvature).

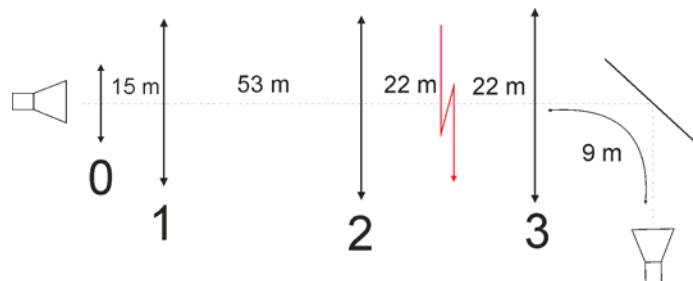


Fig.1. Scheme of the quasi-optical system for microwave diagnostics of the long spark. 0, 1, 2, 3 - lenses.

Table 1 Parameters of the dielectric lenses

№	$D$ , m	$F$ , m	$R$ , m
0	0.2	0.86	1
1	0.9	10.7	12.4
2	0.9	14	16.2
3	0.9	6.7	7.8

**MICROWAVE DIAGNOSTICS OF THE ARTIFICIAL CHARGED AEROSOL CLOUD**

The scheme of quasi-optical system for microwave diagnostics of the artificial charged aerosol cloud is shown in Figure 2, and the lenses parameters are given in Table 2. Calculated width of the microwave beam in the waist is 6 cm.

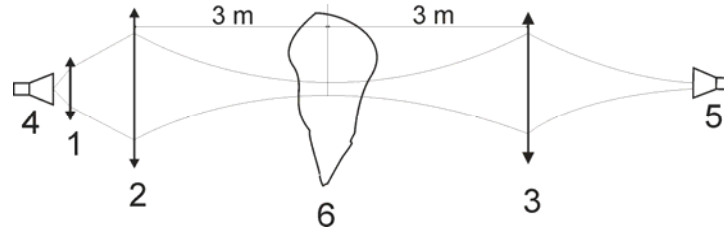


Fig.2 The scheme of quasi-optical system for microwave diagnostics of the artificial charged aerosol cloud. 1, 2, 3 – lenses, 4 - radiating horn, 5 - a microwave receiver, 6 - aerosol cloud.

Table 2 Parameters of the dielectric lenses

№	<i>D</i> , m	<i>F</i> , m	<i>R</i> , m
1	0.2	0.86	1
2	0.5	1.46	1.7
3	0.5	1.46	1.7

**EXPERIMENT**

We were carried out several on measuring of the probing microwave attenuation in the aerosol cloud. In each of these series of experiments quasi-optical system is installed and configured again. Therefore, the position and width of the microwave beam in different series of experiments varied somewhat.

**Experimental setup**

Scheme of experiments is shown in Figure 3. The charged aerosol cloud was formed from the charged steam injected from the nozzle located in the center of the grounded metal disk with a diameter of 2 m. Visual cloud size varied from 1 m to 5 m, depending on the relative humidity of atmospheric air. The average size of cloud drops was 0.5 μm and drop density is about 10<sup>6</sup> cm<sup>-3</sup>. To measure current of upward positive leaders with subsequent spark discharges and synchronization of the recording equipment with discharges a receiving electrode as a metal ball with a diameter of 5 cm was placed on the plane surface of the grounded disk. The top point of the ball rose above the plane of the disk at a distance of 12 cm. The ball was at a distance of 0.7 ÷ 1 m from the center of the disk and joined the measuring shunt (10) with resistance of 1-ohm whose signal was fed to a digital oscilloscope Tektronix DPO with a bandwidth of 500 MHz.

The microwave beam passed through a cloud of approximately normal to its axis (direction of the

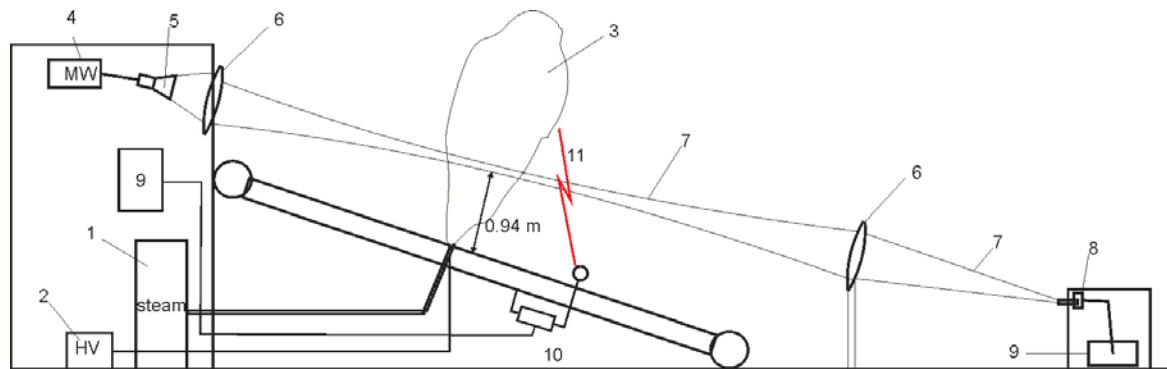


Fig.3. Scheme of the experiment on the investigation of discharges in the charged aerosol cloud by the microwave diagnostic. 1 – steam generator, 2 – high voltage power supply, 3 – charged aerosol cloud, 4 – microwave generator, 5 – horn antenna, 6 – lenses, 7 – microwave beam, 8 – microwave detector, 9 – oscilloscopes, 10 – measuring shunt, 11 – spark discharge cloud-ground.

steam jet) approximately parallel to the ground plane at a distance 0.9 - 1.2 m (in different series of experiments) above the nozzle. The microwaves frequency was 37 GHz, the incident beam power was about 1mW. The relative fluctuation of microwave generator output power was about  $10^{-3}$ . The intensity of microwave radiation passed through the aerosol cloud was registered by a microwave detector with linear characteristics.

IR camera FLIR SC7700M and a photomultiplier FEU-87 (in Figure 4 are not shown) placed about the lens forming the beam (near the horn 5) and were aimed at a cloud at small angles to the direction of the microwave beam –  $8^{\circ}$  and  $10^{\circ}$  correspondingly. The fast optical camera 4Picos is directed at approximately a right angle to the microwave beam (perpendicular to the plane of Figure 4). All devices that were outside of “control room” were placed in metal screens with an autonomous power supply. Synchronization of these devices was made with the use of fiber-optic lines, excluding penetration of electromagnetic interference from discharges into the screens. The typical exposure time of the IR camera was 7 ms. Exposure times for the fast camera 4Picos are shown on the exposure oscillograms in Fig.5a,b (typical exposure time of the first frame was 1  $\mu$ s, the second - 20  $\mu$ s). The time resolution of microwave diagnostics in these experiments was 0.15 microseconds. The optical radiation from the cloud was recorded by the photomultiplier tube FEU-87 in the photon counting mode. Duration of the PMT single photon current pulse was 6 ns. PMT current waveforms listed later in the figures are the average current in the time of 0.1  $\mu$ s. PMT was equipped with an optical system that collects light from a narrow angle - 0.75 rad. PMT was aimed to the region in the cloud above the nozzle of the steam generator through which the microwave beam passed. The size of the visible for PMT region in the cloud was about 5 cm. Time resolution for measurements of the discharge current was 2 ns, it was determined by the bandwidth of the oscilloscope (500 MHz).

The sync pulse time delays in the optical fiber lines, as well as the delays of sync pulse generation by oscilloscope and pulse generator were measured with an accuracy of  $\pm 5$  ns. With the same accuracy the internal delay of 4Picos exposure start is known from passport data. With these delays, as well as the time of propagation of electromagnetic waves from the source to recording equipment, all the experimental

data on the dynamics of various parameters were given to the same time scale.

**Results of the experiments**

A typical set of recorded data for a single discharge event from the last series of the experiments are given in Fig.4 (image obtained with the infrared camera is not presented due to the very weak contrast in this series of experiments). In these experiments positive leaders started from the metal ball usually not

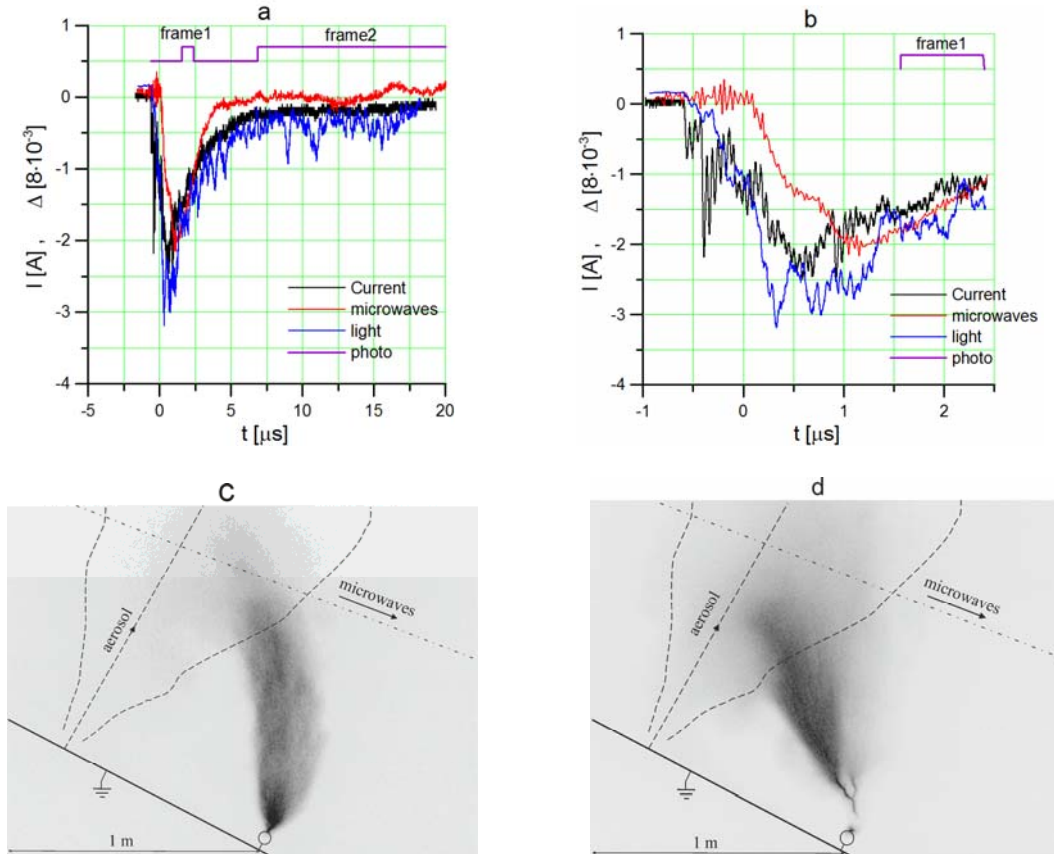


Fig.4 **a, b** – oscillograms of the discharge current  $I$  (black line), relative microwave attenuation  $\Delta$  (red line), the visible light intensity (blew line) and the exposure time of the camera 4Picos (violet line); **c** – the first frame of 4Picos; **d** – the second frame of 4Picos.

reached the cloud and discharges not have the return stroke feature. As can be seen from Fig.4a,b discharge begins with corona flashes from the metal ball - the first two peaks on the oscillogram of the discharge current. PMT at this time registers light of these flashes scattered on the cloud. In 0.7 microseconds from the start of the discharge, the plasma in the cloud appears, recorded by absorption of the probing microwave radiation while increasing the optical emission intensity and discharge current. In the many discharge events the simultaneous sharp growth of discharge current, light emission and absorption of microwave radiation were observed, clearly indicating the relationship of these phenomena. Due to delays in the synchronization scheme we could not run the camera sooner than 1.5 microseconds after the discharge start. By this time, the streamer corona already reaches the clouds – it is observed in all

the first shots by the camera 4Picos (see Fig.4c). It is natural to assume that the ionization in the cloud is evolving under the influence of streamer corona from the metal ball, namely the ionization in the cloud may be either continuation of streamer corona or may develop independently under the influence of enhanced electric field caused by the approach of corona streamers to the cloud.

Approximately at the time of achieving the discharge current maximum (this occurs in 1 to 3 microseconds after the start of discharge) the leader forms near the metal ball and starts moving toward the cloud. As the leader moves away the ball its current decreases monotonically. The lifetime of the leader in different events was from units to tens of microseconds. The optical radiation intensity during the units of microseconds decreases to a level that corresponds to a part of leader discharge radiation scattered from the cloud, and absorption of microwave radiation by the plasma cloud for the same characteristic time completely disappeared.

The second frame of the camera 4Picos had duration of a few tens of microseconds, and began 5-10  $\mu$ s after the discharge start. All these pictures show that the streamer corona of the leader enters the cloud (see Fig.4d). At the same time, the absorption of microwave radiation at this stage is always absent. This means that the average plasma density in the leader corona inside the cloud is low. This effect can be understood from a comparison of the discharge current and the corona form at these two stages of discharge evolution. During the corona flashes and leader formation the discharge current is high, and the corona has the form of a cylindrical jet, part of the cloud (see Fig.4c). During the leader movement its current is low and the corona has the form of a divergent cone. It is obvious that the current density flowing in the cloud at the leader movement stage is much less than at the stage of the corona flashes.

It can be shown that the space-averaged electron density  $n_e^a$  of ionized region in air with the size  $d$  along the microwave beam, which absorbs the part  $\Delta$  of probing microwaves, is equal to

$$n_e^a [cm^{-3}] \approx 3 \cdot 10^{11} \frac{\Delta}{d[m]} \quad (1)$$

From Fig.4c, one can define the size of ionized region in the cloud along the microwave beam, it is approximately equal to 0.3 m. Maximum relative attenuation of the microwave beam has a value  $\Delta = 1.6 \cdot 10^{-2}$  (Fig.4b). Then the maximum value of the space-averaged electron density at the moment shown on Fig.4c can be determined from (1):  $n_e^a \approx 1.5 \cdot 10^{10} cm^{-3}$ .

The presence of non bright discharge channels in the cloud was registered by IR camera in many events. No correlation between the existence of discharge channels and absorption of microwave radiation was observed.

In the previous series of experiments (not presented here) more powerful discharges than described above have been observed. They were longer and had "return stroke" phase - fast and strong ionization of the discharge channel. On the oscillograms of the current the "return stroke" is reflected in the form of sharp and strong current surge (Fig.5). When the spark channel of this discharge crossed the microwave beam, a sharp peak is observed on the oscillogram of the sounding microwave radiation attenuation (Fig.6). Spark channel on the main stage of the discharge (after return stroke) has high conductivity. The characteristic value of the electron density in the channel at this stage is  $\sim 10^{17} cm^{-3}$ . In addition, the channel has a sharp, in relation to microwave radiation wavelength, boundary.

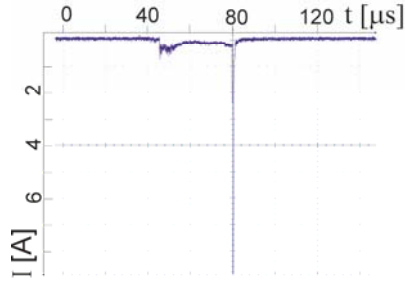


Fig.5 Oscilloscope of the current for discharge with “return stroke”.

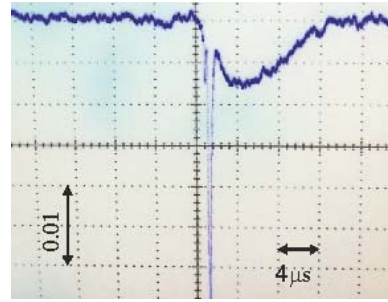


Fig.6 Oscilloscope of the relative microwave attenuation for discharge with “return stroke”.

This channel operates on microwave radiation almost the same as a metal wire. The attenuation of the microwave beam in this case is caused mainly by scattering of microwaves by the plasma channel. Using the solution of the problem of diffraction of a plane electromagnetic wave by a perfectly conducting circular cylinder one can get the following relation for the attenuation of Gaussian microwave beam of radius  $\rho$  crossed by a plasma channel of radius  $a$  along the diameter of the beam:

$$\Delta = \frac{4}{\sqrt{\pi k \rho}} \left[ \left| \frac{J_0(ka)}{H_0^{(2)}(ka)} \right|^2 + 2 \sum_{m=1}^{\infty} \left| \frac{J_m(ka)}{H_m^{(2)}(ka)} \right|^2 \right] \quad (2)$$

where  $J_m$  is the Bessel function of order  $m$ ,  $H_m^{(2)}$  is the Hankel function of the second kind of order  $m$ ,  $k = \omega/c$  is the wave number. The maximum observed value of the relative attenuation of the microwave radiation by the spark channels is equal to 0.09. Assuming that in this case the plasma channel crossed the microwave beam along its diameter, and taking the value of the beam radius  $\rho \approx 4$  cm one can determine the diameter of the plasma channel from the equation (2). It is equal to 2 mm, which agrees well with the known data on the diameter of the spark channels.

## CONCLUSIONS

The results of the experiments in this study proved the effectiveness of the use of microwave diagnostics in investigation of spark discharges, including those arising in the charged aerosol cloud. The microwave diagnostics allowed us to measure the absolute value and the dynamics of the average conductivity in the cloud. These parameters can not be obtained by the experimental methods traditionally used in studies of sparks and lightning. It can be expected that the application of the microwave diagnostics to the long spark research will be also fruitful.

## ACKNOWLEDGMENTS

This work was supported by the Russian Government (contract No. 14.B25.11.0023).

## REFERENCES

- Les Renardieres Group, 1977: Positive discharge in long air gap at Les Renardieres – 1975 Results and Conclusions. *Electra*, 53, 31-151.